Drop-Size Distributions Produced by Turbulent Pipe Flow of Immiscible Liquids

S. B. COLLINS and J. G. KNUDSEN

Oregon State University, Corvallis, Oregon

Drop-size distributions in turbulently flowing dispersion of immiscible liquids were investigated. The observed drop-size distributions were actually a composite of two superimposed distributions. One is the distribution produced by the injection nozzle and the other is that produced by breakup in the turbulent flow field. A mathematical model was developed which predicted both the shape of the observed distributions and kinetics of the droplet breakup process for the distribution produced by the turbulent flow field.

The flowing dispersion composed of water and insoluble organic phase was photographed at 27, 209, 421, and 576 pipe diameters below the mixing jet and at distances of 0.05, 0.1, and 0.4 diam. from the wall. Average flow rates varied from 14 to 20 ft./sec. in the 0.750-in. I.D. tube. Three organic phases were studied at concentrations ranging from 0.6 to 10% by volume. Dispersed phase viscosity and interfacial tension varied from 1 to 18 cp. and 13 to 40 dynes/cm.

No distribution law with any theoretical basis could be found which correlated experimental distributions.

The stochastic model describing the breakup process postulates that each breakup event leads to two daughter drops with uniformly distributed volume ratios and a very small satellite droplet. An empirical correlation exists to predict only one of the three parameters of the model.

Rational design of dispersed phase reactors and other dispersed phase contacting equipment requires a knowledge of the drop-size distributions. Previous studies of breakup in definable fields of flow have been directed toward determining the factors influencing droplet breakup. An important result of these studies was the demonstration of the existence of a critical drop diameter below which drops are stable. Drop-size distributions have been measured previously only in flow systems containing ill-defined and variable regions of turbulence.

The difficulties involved in measuring size distributions are probably responsible for the sparsity of experimental data. In the present paper a previously developed (*11*) photographic technique is used for the measurement of the drop-size distributions resulting from the action of the turbulent field produced during pipe flow. The distributions are examined by means of a mathematical model, and the nature of the mechanism of breakup is postulated.

BACKGROUND DISCUSSION

The splitting of liquid droplets while residing in various flow fields has been considered both theoretically and experimentally. Rumscheidt and Mason (*9*) observed three classes of droplet distortion for couette flow: a sigmoidal shape with droplets released from the pointed ends, a dumbbell-shape with rapid thinning of the neck until breakup occurred, and a spheroidal shape that did not lead to fracture.

Clay (*2*) studied both breakup and coalescence of droplets in turbulent fields. He proposed that drops could burst in a turbulent field by three possible mechanisms: laminar shear, turbulent shear, and turbulent pressure fluctuations.

Hinze (*4*) considered the breakup of drops in an air stream and emulsification in a turbulent field and classified the deformation of drops into three types: lenticular or disc-shaped resulting from centrifugal forces on a rotating drop, elongation of the drop, and bulgy deformation as proposed earlier by Clay. Hinze supposed all three types of deformation were present in a turbulent field but that elongation deformation was probably most prevalent.

Kolomogorov (*6*) and Hinze independently developed the same expression for the critical Weber number of breakup in turbulent flow by dimensional arguments. Hinze showed that in isotropic homogeneous turbulence

$$(N_{we})_{\text{crit}} = C[1 + \psi(N_{Vi})] \tag{1}$$

and

$$\overline{v^2} = C_1(\varepsilon D_{\max})^{2/3} \tag{2}$$

thus when N_{Vi} [and hence $\psi(N_{Vi})$] approaches zero, the following expression results from Equations (1) and (2):

$$D_{\max}(\rho_c/\sigma)^{3/5}\varepsilon^{2/5} = C_2 \tag{3}$$

Clay performed experiments on emulsion formation in turbulent flow fields under two different conditions, in the turbulent field of flow in the space between two coaxial cylinders and in a flow loop constructed from 4-in. pipe. He observed very few distorted drops and was lead to favor the turbulent pressure fluctuation mechanism for droplet breakup.

Hinze rearranged Equation (3) into the form

$$\frac{\rho_c \sigma D_{95}}{\mu_c^2} = 0.725\left(\frac{\mu_c^5\,\varepsilon}{\rho_c \sigma^4}\right)^{-2/5} \tag{4}$$

and found that this equation fit Clay's data quite well. However, Sleicher (*10*) pointed out that the comparison was based on data representing a wide range in physical properties and very small range in droplet diameters.

Sleicher measured the Reynolds number which caused only 20% of a group of equal diameter drops to break up in a turbulent field. He called this diameter the maximum stable drop diameter $D_{\max}$ for the corresponding Reynolds number.

In every case he had observed breakup only very close to the wall where the turbulence was least homogeneous and least isotropic. In high-speed motion pictures of drops moving 15% faster than required to make them unstable, two types of breakup were seen. The most prevalent was breakup into two approximately equal drops. A second

breakup mechanism resulted in the stripping of a small drop from a larger one. This type of breakup was less frequent than the first and Sleicher thought it improbable for a marginally unstable drop.

To account for dispersed phase viscosity effects, Sleicher used the form of Equation (1) to obtain

$$\frac{D_{\max}\rho_c U^2}{\sigma}\sqrt{\frac{\mu_c U}{\sigma}} = 38\left[1 + 0.7\left(\frac{\mu_d U}{\sigma}\right)^{0.7}\right] \qquad (5)$$

This equation correlated all the data within 35%. A subsequent study by Paul and Sleicher (*8*) revealed that coefficient in Equation (5) was proportional to the 0.1 power of the pipe diameter.

Description and Measurement of Drop Sizes and Drop-Size Distributions

Empirically a size distribution can be found by dividing the size range of a population of drops into a number of increments and determining the number which fall into each interval. A plot of the fraction of the total count found in each interval against the average size of the particles in the interval gives a frequency diagram or histogram. In the limit, as the number of particles becomes very large and the size of the increments very small, the histogram becomes a continuous curve.

Mugele and Evans (*7*) proposed the general equation for various average drop diameters:

$$D_{qp}^{q-p} = \int_0^\infty D^q f(D)\,dD \Big/ \int_0^\infty D^p f(D)\,dD \qquad (6)$$

$$(q > p; \quad q = 1,2,3; \quad p = 0,1,2)$$

Measurement of Drop-Size Distributions

Drop-size distribution is one of the most difficult properties of a dispersion to predict theoretically or to measure experimentally. A variety of experimental techniques has been devised by previous investigators, but no one method has been found which allows the rapid accurate determination of drop-size distributions containing a wide range of diameters.

Direct photography of a flowing liquid-liquid dispersion has been employed by several investigators. Kinter et al. (*5*) presented a review of many techniques of photography which had been adapted to bubble and drop research. Large drops (diameter > 200 μ) at low concentration present no inherent photographic difficulties.

Ward (*11*) pointed out that the following difficulties arose when concentration increased and drop size decreased: (1) light transmittance decreases; (2) magnification by the camera magnifies drop speed requiring shorter exposure time; (3) drop images may be distorted by drops between lens and plane of focus. He developed an apparatus which allowed him to photograph drops (diameter 1 to 800 μ) in dispersed phase concentrations up to 50% by volume flowing at velocities up to 16 ft./sec.

Elimination of the long, tedious effort needed to obtain drop-size distributions from photographs has also received some attention. Adler et al. (*1*) used the sweep of a narrow light beam and a photocell to measure drop-size distributions from photographic negatives. Until this obstacle is overcome, laborious measurement of large numbers of individual droplets from photographs appears to be the best method available for the determination of drop-size distribution of unstable liquid-liquid dispersions.

EXPERIMENTAL PROGRAM

The primary goal of the study was to characterize the drop-size distributions formed when a liquid-liquid dispersion was exposed to turbulent pipe flow. Previous investigators (*2*, *11*) have determined distributions in turbulent flow systems, but the test apparatus has included pumps, tanks, and pipe fittings, all of which have unknown effects on the distribution. In the present work, the change in drop size and distribution during pipe flow is studied at various locations downstream from the injection of the immiscible liquid. The drop-size distribution existing at the injection point is characteristic of the injection nozzle itself but subsequent changes are probably due to turbulence.

A summary of the experimental conditions under which distributions were measured is given in Table 1. Tap water was used as the continuous phase in all cases. Three organic phases with viscosity ranging from 1 to 17 cp. and interfacial tension ranging from 13 to 40 dynes/cm. were used. The majority of the measurements were made with Shellsolv, a kerosene-like solvent, which had a viscosity of 1 cp. and an interfacial tension of 40 dynes/cm. The physical properties of the liquids are shown in Table 2. After each run the clear liquids were separated discarding any sludge that had accumulated at the interface. Fresh tap water was used for each run. Properties of the three dispersed phase liquids were measured periodically and remained unchanged even though reused.

EXPERIMENTAL APPARATUS

The apparatus was designed to produce through turbulent pipe flow an unstable dispersion of immiscible liquids and to allow the dispersion to be photographed at intervals along the length of the pipe as well as at varying distances from the pipe wall. Separate pumping of the water and organic phases was provided to eliminate dispersion caused by the high shear rates in a pump. Flanges in the test section allowed the observation window to be mounted at various locations along the length of the test section. The narrow focal plane of the camera lens system located a sufficient distance from the lens surface permitted photographs to be taken at varying distances from the tube wall.

Water at a measured flow rate was pumped to the vertical test section from a Tygon-coated storage and settling tank. A small gear pump with a by-pass line provided a stable, easily controllable flow of organic phase from a small stainless steel tank to the mixing jet. Two mixing jets of ¼- and 3/16-in. O.D. were constructed from thin wall stainless steel tubing. A 9½-in. section of 0.745-in. I.D. transparent plastic pipe was installed in place of the brass test section to facilitate centering the jet in the test section.

The test section consisted of lengths of 0.875-in. O.D. by 0.745-in. I.D. brass tubing connected by self-aligning flanges which permitted the discontinuity of the tube wall to be held below 0.001 in. at the joint. The flange system permitted photo-

TABLE 1. SUMMARY OF THE EXPERIMENTAL PROGRAM

Dispersed phase (Run CODE)	Conc., vol. %	Nozzle size, in.	Flow rate, ft./sec.	Linear position*				Radial position (y/R_w)		
				3	2	1	B	0.05	0.1	0.4
Shellsolv										
1SS	0.6	3/16	14			x				x
2SS	0.6	3/16	16	x		x		x	x	x
3SS	0.6	3/16	20			x			x	
4SS	1.3	3/16	14			x			x	x
5SS	1.3	3/16	16	x	x	x	x	x	x	x
6SS	1.3	3/16	18			x			x	x
7SS	1.3	3/16	20	x				x	x	x
7SS	1.3	3/16	20			x			x	x
8SS	5	3/16	16	x				x	x	x
8SS	5	3/16	16		x					x
8SS	5	3/16	16				x		x	
9SS	1.3	1/4	16	x	x	x			x	x
10SS	5	1/4	16	x				x		
10SS	5	1/4	16		x			x	x	
10SS	5	1/4	16			x			x	x
10SS	5	1/4	16				x		x	
11SS	10	1/4	16	x	x			x	x	
11SS	10	1/4	16			x		x	x	x
11SS	10	1/4	16				x	x		x
Light oil						x				x
1LO	0.6	3/16	16	x				x		
1LO	0.6	3/16	16		x			x		x
2LO	5	3/16	16	x			x	x	x	
2LO	5	3/16	16		x			x		x
Iso-octanol										
1OA	0.6	3/16	16	x			x	x	x	x
2OA	1.3	3/16	16	x			x	x	x	x
2OA	1.3	3/16	16		x			x		x
3OA	5.0	3/16	16		x			x		

*Distances from the injection nozzle to the window were as follows: 3–27.1 pipe diameters; 2–209 pipe diameters; 1–421 pipe diameters; B–576 pipe diameters.

Table 2. Physical Properties

Temperature, °F.	Shellsolv		Light oil		Isooctyl alcohol	
	Density, lb./cu. ft.	Viscosity, cp.	Density, lb./cu. ft.	Viscosity, cp.	Density, lb./cu. ft.	Viscosity, cp.
66	49.0	1.2	54.1	16.4	53.1	9.7
68	48.8	1.1	54.2	15.6	53.0	8.6
70	48.8	0.1	53.8	14.7	53.0	8.7
74	48.8	0.97	53.7	13.9	53.0	8.3
Interfacial tension, dynes/cm.						
68	40.3		17.6		13.0	

graphs to be taken at 27.3, 209, 421, and 576 diam. below the mixing jet.

The discharge of the return leg was located under the surface of the liquid in the storage tank. Thus a constant net head was maintained on the pump as the liquid level raised in storage tank A, and a stable overall flow rate resulted.

The observation window is shown in detail in Figure 1. The design minimized flow disturbance and eliminated leakage at high operating pressure. The section was constructed by casting a block of polyester resin around the middle of a 10-in. piece of test section tubing. After the plastic hardened, an endmill was used to machine ¾-in. diameter flat bottom holes in opposite sides of the block to a depth sufficient to create slots 3/16 in. wide on opposite sides of the tube. Glass discs ¾ in. in diameter and 1/16 in. in thickness cut from microscope slides were inserted in these holes. Rubber O-rings and plastic retaining rings secured by screws completed the section. The maximum discontinuity at the wall was 0.010 in. The resulting assembly was leak free with an internal pressure of 75 lb./sq. in.

Photographs of the dispersion were taken with a Hasselblad Model 1000F single lens reflex camera equipped with an 80-mm. lens and a 100.2-cm. extension tube. The resulting optical system produced an image approximately 12 times actual size on the film and had a depth of focus of approximately 1,500 μ. The camera and extension tube were rigidly mounted on a sliding table of a heavy cast iron base. The position of the table with respect to the base was measured with a dial indicator graduated in 0.005-in. divisions.

Backlighting of the dispersion was accomplished by means of a General Radio Strobotac Model 1531A strobe light. For concentrations above 5% a Bell and Howell 3-in. f2 projection lens was used between the strobe and the window to concentrate the light on the dispersion.

EXPERIMENTAL PROCEDURE

A typical experiment was begun by pouring a small amount of the organic phase into the bottom of the large storage tank and then filling the tank with approximately 300 gal. of tap water.

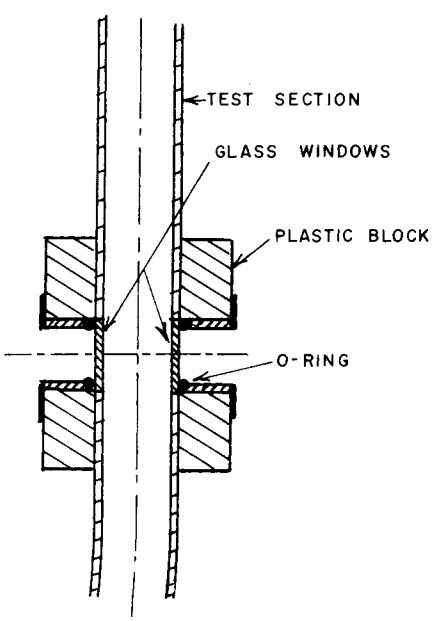

Fig. 1. Cross section of observation window.

Final adjustment of the water temperature was accomplished by frictional heating to bring the temperature to 68° ± 1°F. Flow rates were adjusted and pictures were taken during a 10-min. period before the entrained organic phase began to pass through the water pump.

One complete roll of 13 pictures was taken at each set of experimental conditions. This was usually sufficient to yield samples of 250 drops in focus which were measured with a transparent plastic ruler which was graduated to read directly in 25-μ increments. Since the decision as to which drops were in focus and which were not was somewhat subjective, all of the measurements were made by one person. In the case of distorted drops, all diameters were measured parallel to one another such that the diameter appeared to bisect the area of the drop. The random orientation of the drops thus eliminated biasing of the measurements.

EXPERIMENTAL RESULTS

The drop-size distribution at a given position is produced from a distribution originally created upon injection at the nozzle and under the influence of turbulence between the point of injection and the point of observation. The results were analyzed to determine the effect of turbulence alone.

Attempts were made to find a distribution law which would describe the drop-size distributions so that comparison of the distributions could be accomplished by noting the changes in the parameters of the distribution instead of the more cumbersome visual comparison of the distribution curves themselves.

The inadequacy of the log-normal distribution law is best illustrated by a log-probability plot of a representative set of data shown in Figure 2. As the mixture flows through the pipe, the distribution is increasingly divergent from the log-normal type. Extrapolation to the nozzle would indicate nearly log-normal distribution at that point, but the action of turbulence was not to generate a log-normal distribution.

No adequate distribution law was found and the data were presented and compared in graphical form. Although the distributions were not log-normal, log-probability plots of the distributions were found to be very useful for comparative purposes. Complete distributions and average size data are available (3).

Possible errors fall into two broad classes: empirical and

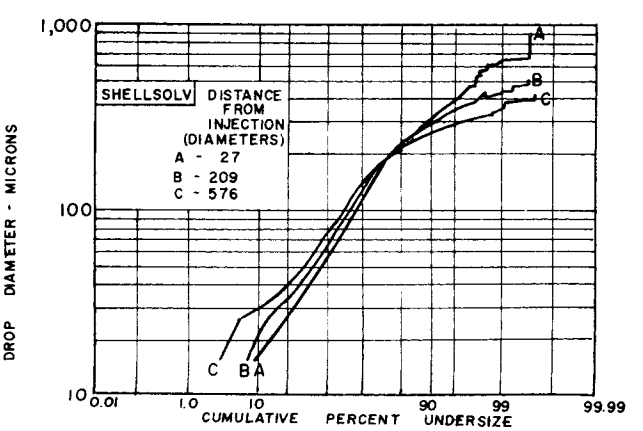

Fig. 2. Drop-size distributions (number frequency). 1.3% Shellsolv; $y/R = 0.1$; $V = 16$ ft./sec.

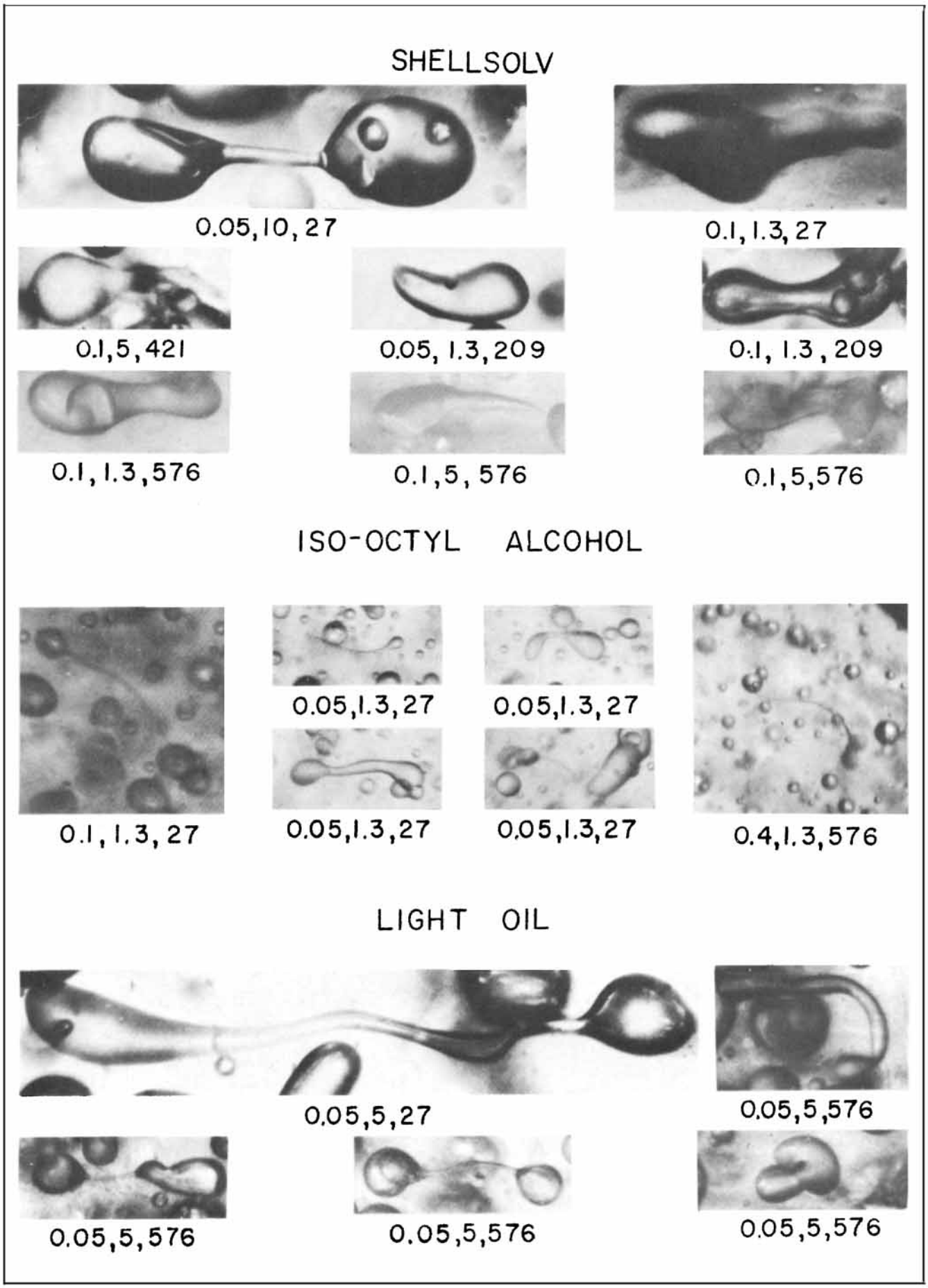

Fig. 3. Highly deformed drops (×32). Numbers under pictures are, respectively, y/R, concentration, and number of diameters from injection point. Velocity is 16 ft./sec.

statistical. Empirical errors arise from uncertainties in the experimental conditions but were probably largely due to variations in picture quality. Deterioration in picture quality was caused in most cases by the increase in distance between the camera focal plane and the wall of the pipe. The quality of the pictures was subjectively graded into four classes. Class A photographs were judged very sharp and easy to process. Class D photographs were difficult to evaluate and the distributions obtained from them were of questionable value. The primary effect of poor picture quality was to bias the distribution toward large drops.

An idea of the reproducibility of the data was obtained by duplicating runs on dates separated by a period of three months. In one case, a sample size of 278 drops was used. In the duplicate case, a sample of 1,309 drops was used. Identical distributions were obtained. These results also indicated that a sample size of 250 drops was sufficient.

A composite photograph of highly deformed drops observed under a variety of experimental conditions is shown in Figure 3. The drops shown were chosen to illustrate the modes of deformation observed and the variety of conditions under which deformation occurs. The most highly deformed drops appear dumbbell-shaped with two relatively large globules of liquid connected by a thin filament of liquid. What appear to be fragments of drops photographed shortly after the rupture of the thin filament were also observed. Highly deformed drops were much more prevalent when isooctyl alcohol or light oil was the dispersed phase. This was probably a result of the higher dispersed phase viscosity of these two liquids, which logically would increase the time scale of the breakup process. The probability of photographing the breakup process would then increase.

In the nearly 1,300 prints examined during this study no indications of coalescence were observed. Two possible explanations for this are that the coalescence happens extremely fast or that it occurs very infrequently. Two mechanisms for coalescence have been proposed by Clay (*2*). The first was a rapid direct coalescence in which a small impinging drop merges almost instantaneously with a larger drop. A rough calculation shows that with a flash duration of approximately 1 μsec. a 50-μ drop would have to be traveling about 10 times faster than the average velocity of the liquid in the tube if it were not to be seen entering the profile of the larger drop. Such velocities do not seem likely. The second proposed mechanism was a slower process in which two drops cling together, the continuous phase between them drains away, and the drops merge. Clay states that one or more small drops were seen clinging to a larger drop very often in his photographs, whereas highly deformed drops were never seen. The fact that Clay observed coalescence and they were not observed during the present study using comparable flash deviations rules out the second process fairly decisively. Thus it was concluded that coalescence phenomena could be legitimately neglected in the present study and that the drop-size distributions observed were characteristic of the breakup process alone.

Coalescence may also have been inhibited because of low concentrations of the dispersed phase, by additives derived from the polymeric coatings in the systems, and by the use of tap water as the continuous phase. The dispersion, however, coalesced rapidly when at rest in a container.

The relative distortion of the drops was subjectively graded. High deformation and (presumably breakup) appeared to be much more probable close to the wall in the buffer layer than in the turbulent core. This result is in agreement with Sleicher's (*10*) observation that drops tended to break up in the wall region of the pipe. The general trend is for larger values of D_{32} in the turbulent core region than in the buffer layer. However, the differences were small and often masked in experimental error so no quantitative conclusions can be drawn.

Distributions for 1.3% by volume Shellsolv with an average linear velocity in the tube of 16 ft./sec. are shown in Figures 2 and 4. The distributions observed at the same radial position in the pipe seem to intersect at a common point. This behavior was observed in almost all cases, although the point of intersection varied widely with the system under consideration.

The effects of concentration and nozzle size were strongly coupled and difficult to separate. Figures 2, 5, and 6 illustrate typical results obtained as dispersed

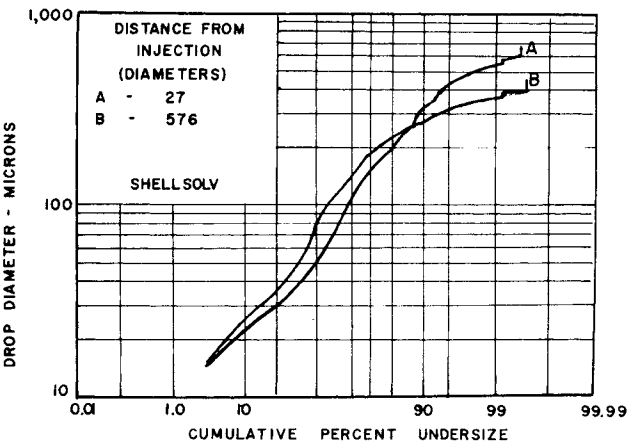

Fig. 4. Drop-size distributions (number frequency). 1.3% Shellsolv; $y/R = 0.4$; $V = 16$ ft./sec.

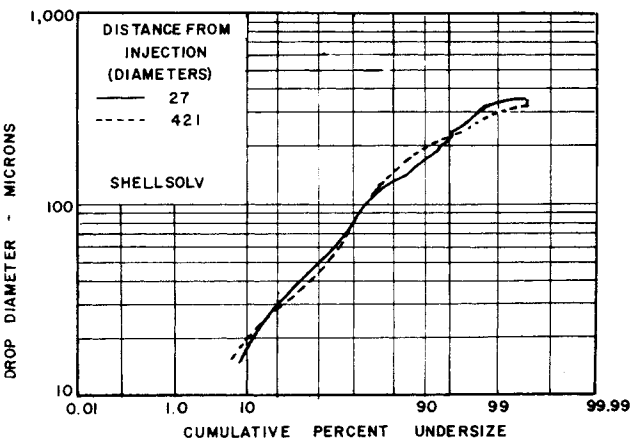

Fig. 5. Drop-size distributions (number frequency). 0.6% Shellsolv; $y/R = 0.1$; $V = 16$ ft./sec.

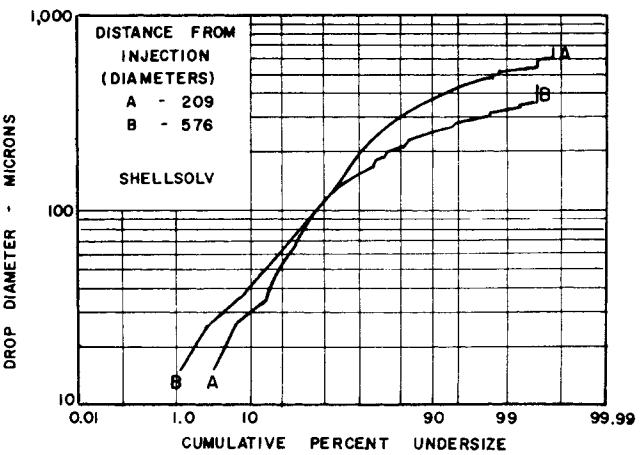

Fig. 6. Drop-size distributions (number frequency). 5% Shellsolv; $y/R = 0.05$; $V = 16$ ft./sec.

phases concentration was increased from 0.6 to 5% by volume. Concentration and nozzle size primarily affected the initial distribution observed 27 diam. below the inlet. At 0.6% by volume dispersed phase, only 5% of the drops measured had diameters above 230 μ, the maximum stable drop size as predicted by Sleicher's correlation, Equation (5). Figure 5 indicates that little breakup occurred at this concentration, which is not surprising in view of the small number of unstable drops present. For concentrations of 1.3 and 5%, the percentages of drops with diameters greater than 230 μ were 19 and 22%, respectively. Considerable breakup is evident in Figures 2 and 6.

The distributions all have the same form for varying velocity. The mechanism of breakup appeared to remain the same over the range of average velocities between 14 and 20 ft./sec. The distributions at various distances from the nozzle indicate that this change is a result of a change in the distribution produced by the nozzle and not a change in the breakup mechanism.

Figure 7 shows distributions obtained for a light oil system. The distribution for curve *B* is shifted about 15% to the left of the position which would be expected from the Shellsolv results. These results were obtained from poor quality prints, so one plausible explanation for this shift would be that the distribution was biased toward large drops by poor print quality. The form and position of distributions given by curves *A* and *C* were reproduced quite well by duplicate runs and were therefore judged to be representative of the system.

Figure 8 is representative of the results obtained for the isooctyl alcohol system. The most noticeable change in the distributions was the shift in the point of intersection of the distribution toward the range of small drops.

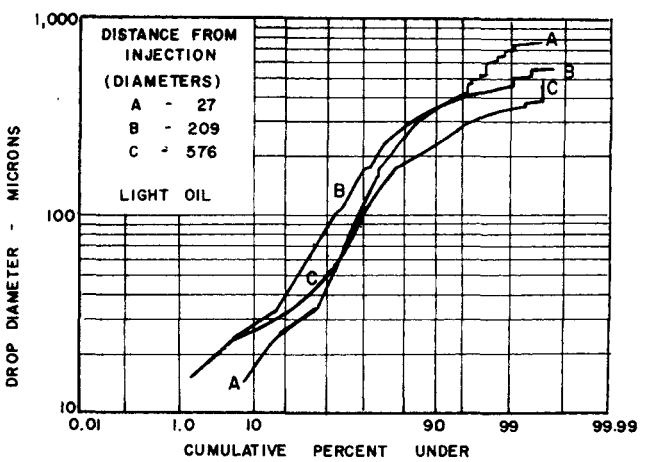

Fig. 7. Drop-size distributions (number frequency). 5% light oil; $y/R = 0.05$; $V = 16$ ft./sec.

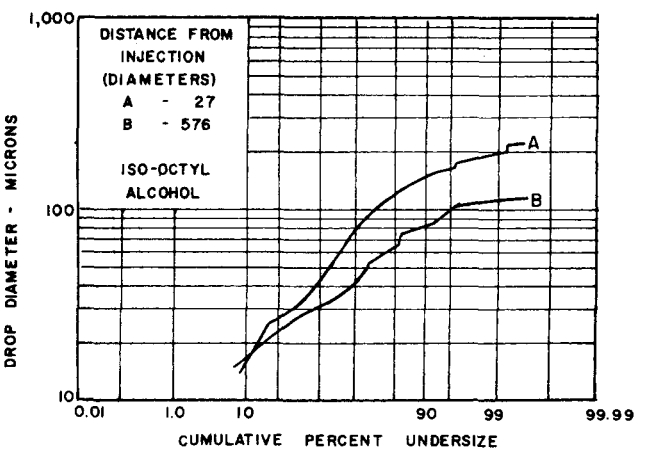

Fig. 8. Drop-size distributions (number frequency). 1.3% isooctyl alcohol; $y/R = 0.1$; $V = 16$ ft./sec.

DISCUSSION OF RESULTS

Mathematical Model

Possible mechanisms were explored and expressed quantitatively in order to develop a model of droplet breakup for the systems. The stochastic approach as opposed to the deterministic approach to mathematical modeling was indicated by the chaotic nature of the turbulent field responsible for breakup as well as the large number of breakups leading to the observed distributions.

Because of the low dispersed phase concentrations (less than 10%) used in the experiments and the short time (less than 3 sec.) during which the dispersion was in the pipe, coalescence effects were considered negligible compared to breakup. As pointed out previously, no coalescence was observed, while a significant number of highly deformed drops which appeared ready to fracture and likewise fragments from such fractures were noted.

Central to the proposed model is the postulate that the entire process may be considered to take place in independent discrete steps. As described earlier, previous workers (*8, 10*) have shown both experimentally and theoretically the existence of a maximum stable drop size for liquid-liquid dispersions in turbulent pipe flow. Thus any model would be expected to include the maximum stable drop size as a parameter. These two ideas, together with the requirement that the total mass of the dispersed phase must be conserved, were used as starting points in the evolution of the model.

Actual implementation of the model was in the form of a FORTRAN program employing Monte Carlo techniques. Figure 9 shows a generalized flow chart for the subroutine model. Previous to this subroutine, the distribution under consideration has been stored in an original array. The random nature of the breakup process was simulated with the aid of a random number generator. For example, if it was postulated that there was a 50% chance of breakup, a random integer between 0 and 99 was generated from a uni-

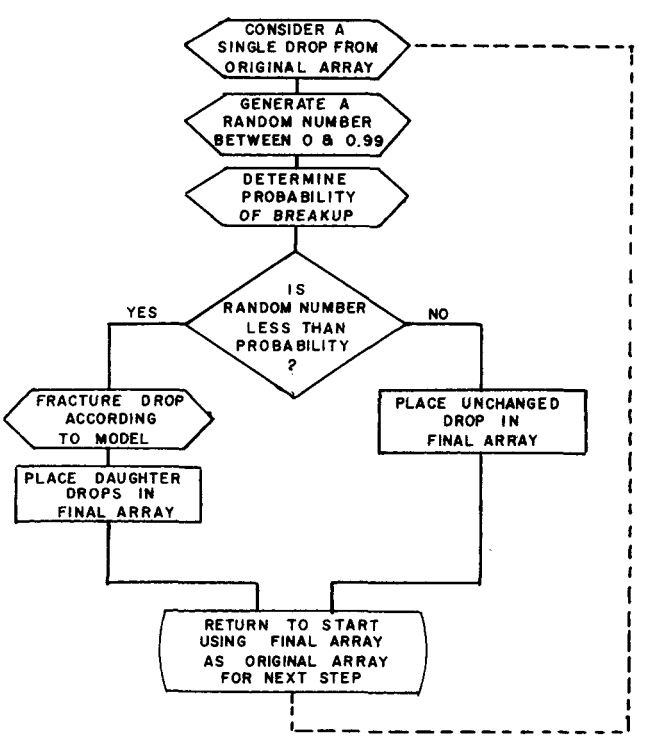

Fig. 9. Generalized subroutine for model.

form distribution. If the random number generated was greater than or equal to the probability of breakup, breakup did not occur. If the number was less than the probability, breakup occurred. In most of the models a random number generator was also used to randomize the size of the daughter drops resulting from breakup. Uniform populations and normal populations were used for this purpose. Drops resulting from the breakup process were placed in a final array. After all of the elements of the original array had been considered, the contents of the second array became the original array for the next step and the process was repeated. A summary of the various models investigated is given in Table 3.

Proposed models were judged by their ability to simulate the experimental distributions observed downstream, when the distribution observed at the injection point was used a beginning array for the program. Experimental distributions were compared graphically by number frequency versus diameter histograms and log-probability plots and numerically by comparison of average diameters.

An investigation of all proposed models showed that model 11 predicted a sequence of distributions very similar in form to those observed experimentally, and it was concluded that this model gave an adequate qualitative representation of the events occurring in the pipe.

The reason no simple size-distribution law could be found to describe the experimentally observed distribution is obvious from the form of the model. The existence of the maximum stable drop size means that the portion of the initial distribution with diameters less than maximum stable drop size remains unchanged by the action of the turbulence. Thus as mentioned, what was actually measured was a superposition of two distributions, one initially present and the other produced by the turbulence.

Once a qualitatively correct mathematical model had been developed, a quantitative comparison of the average sizes [Equation (6)] calculated from theoretical and experimental distributions was made. Model 11 is a three-parameter model and such comparisons allowed a set of parameters to be determined. The three parameters are: (1) D_{max}, the maximum stable drop diameter; (2) $D_{1.0}$, the drop diameter at which probability of breakup becomes one; (3) R_v, the range of volume ratio of satellite to daughter drops (that is, when $R_v = 0.02$ the range of satellite to daughter drop varies uniformly between 0 and 0.02).

TABLE 3. MATHEMATICAL MODELS EXAMINED

Model	Description
1	All drops have a 50% probability of breakup into two daughter drops having a uniformly distributed volume ratio.
2	Same as model 1 except that the ratio of daughter drop volumes is distributed normally about 0.5.
3	All drops with a diameter greater than D_{max} have a 50% probability of breakup into two uniformly distributed daughter drops.
4	Drops with diameters below D_{max} have a 10% chance of breakup; those with diameters above D_{max} have a 50% chance of breakup. A pair of uniformly distributed daughter drops result from each breakup.
5	Drops with diameters above D_{max} have a 50% chance of breakup into three equal daughter drops.
6	Drops with diameters above D_{max} have a 50% chance of breakup. Two to six equalized daughter drops are produced with equal probability.
7	Drops with diameters above D_{max} have a 50% chance of breakup into a pair of uniformly distributed daughter drops and a single small satellite drop whose volume is a fixed fraction of one of the daughter drops.
8	Same as model 7 except two satellites are formed.
9	Probability of breakup is zero below a diameter equal to D_{max} and increases linearly to a 1.0 probability at a diameter equal to $D_{1.0}$. Two uniformly distributed daughter drops and a satellite drop of fixed volume ratio are produced.
10	Same as model 9 except probability increases quadratically.
11	Same as model 9 except the satellite to daughter drop volume ratio is uniformly distributed over a fixed range.

The first two parameters define the probability of breakup of an individual drop. If the diameter is less than D_{max}, the probability of breakup is zero. If the diameter is greater than $D_{1.0}$ the probability of breakup is unity. If $D_{max} < D < D_{1.0}$ the probability of breakup is a linear function of diameter. For probabilities between 0 and 1 a random number is generated to determine if breakup occurs or not.

The model should predict not only the correct individual distributions, but also the proper sequence of distributions or kinetics as the dispersion flows through the pipe. In order to test this aspect of the model a plot of experimental values of D_{32} versus distance from the nozzle was made, as shown in Figure 10. The values of D_{32} predicted by the model can be compared with the experimental values by constraining the experimental and theoretical curves to match at the nozzle and at a point close to 576 diam. from the nozzle. With these two points fixed, the remaining theoretical points can be plotted by interpolation assuming that the time between each breakup step is constant. The results of such a plot for the data from the 1.3% Shellsolv system used earlier to develop the model is shown in Figure 10. The best set of parameters predicts average sizes which differ no more than 10 μ from those measured experimentally. The set of theoretical distribution curves and a theoretical histogram resulting from the best set of parameters are shown in Figures 11 and 12 and adjacent plots show the experimentally determined results. In Figure 12 the solid line is the same in each plot representing the distribution 27 diam. from injection and the initial array used in the model.

Similar analyses of the data from a 5% light oil system (Figure 8) and a 1.3% isooctyl alcohol system (Figure 9) were also performed. The agreement of the experimental and theoretical kinetics for the light oil and the isooctyl alcohol systems are also shown in Figure 10. The theoretical distributions are in good qualitative agreement with the experimental observations shown in Figure 8 and 9 in both cases. Although no attempt was made to find the optimum parameters for the other sets of experimental data, the

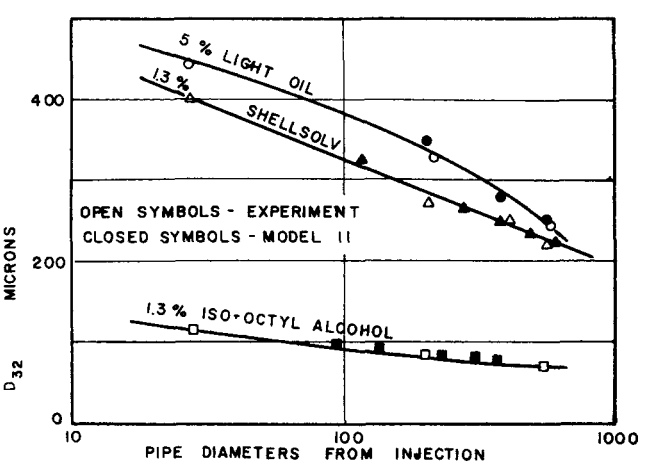

Fig. 10. Variation of D_{32} with distance from injection nozzle. Predicted values used the following parameters:

	D_{max}	$D_{1.0}$	R_v
Shellsolv	200	700	0.01
Light oil	150	1,250	0.02
Isooctyl alcohol	100	140	0.05

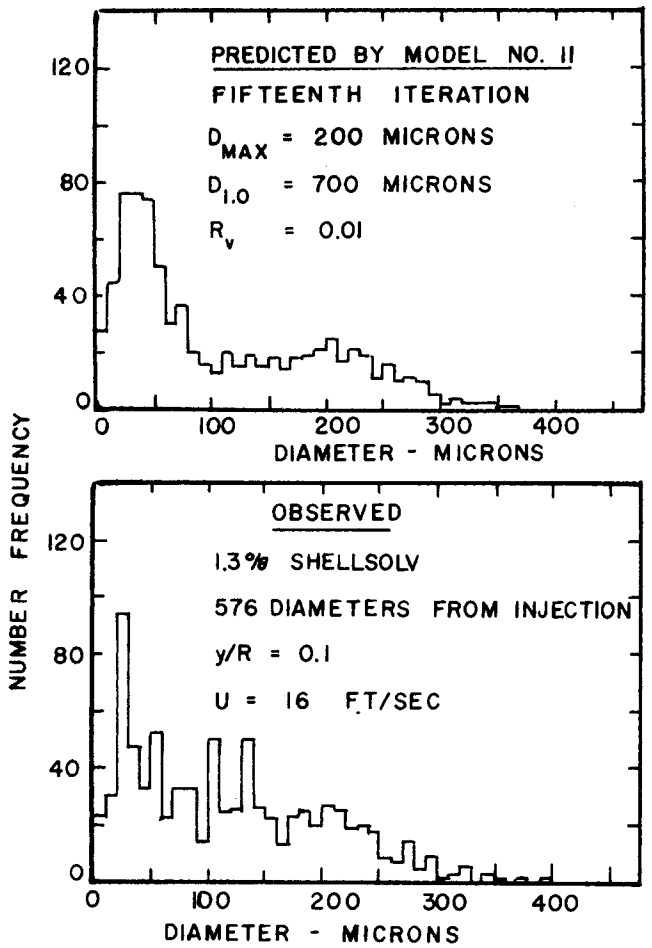

Fig. 11. Predicted and observed histograms.

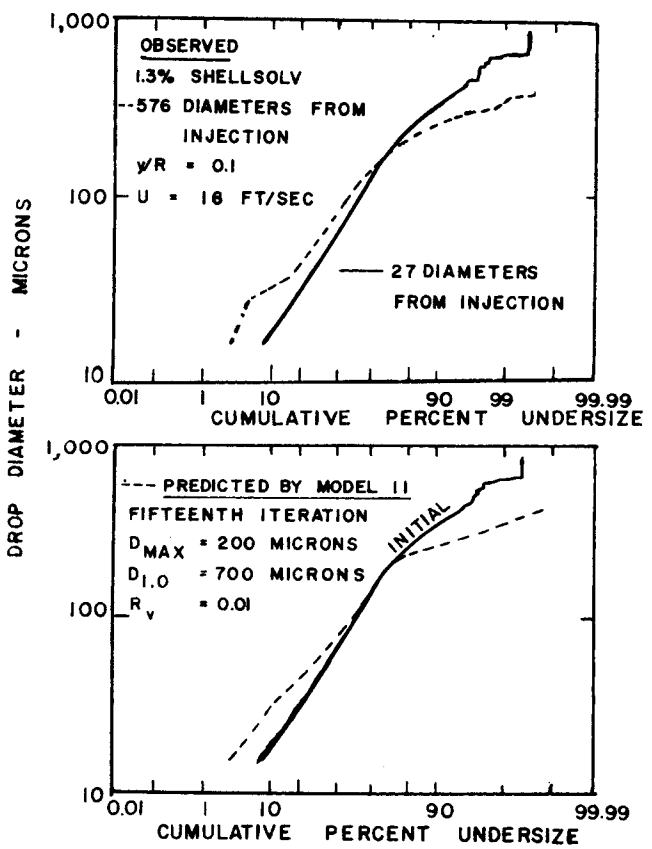

Fig. 12. Predicted and observed drop-size distributions. The solid curve is identical on each plot.

similarity to those which were treated would indicate that no fundamental change in the model would be necessary to achieve a good fit in all cases.

The agreement between the maximum stable drop size as predicted by Sleicher's correlation and that predicted by the model is very good. Equation (5) gives maximum stable drop size of 214, 157, and 90 μ for the Shellsolv, light oil, and isooctyl alcohol systems, respectively. Best results with the model were obtained with corresponding maximum stable drop size of 200, 150, and 100 μ. The differences are within the ±35% claimed for the correlation. No correlation exists for the prediction of the other two parameters of the model.

Although uniqueness of the breakup mechanism proposed in the model developed during the course of the present work cannot by proven, the agreement between theory and experiment provides evidence that the proposed mechanism is a reasonable one for breakup in the turbulent field of a pipe.

Since it is a three-parameter model, it is probably not the only one which will fit the experimental data. According to the model, when drops break up in the turbulent core of a pipe, two daughter drops are produced which have uniformly distributed volume ratios. On the average, one very small satellite drop is also produced by each breakage event. The effects of a maximum stable drop size were clearly present in the experimental data by comparing the predictions of models 1 and 3 which did and did not postulate the existence of a maximum stable drop size. Pure binary and higher order breakup mechanisms were also eliminated as possible mechanisms in the other models.

CONCLUSIONS

1. Drop size and drop-size distributions were determined for liquid-liquid dispersions flowing turbulently in a circular tube. The observed distributions are two superimposed distributions, the distribution produced by the injection nozzle and the distribution produced by the turbulence of the flowing stream.

2. There are indications that the distribution of droplets produced at the nozzle is log-normal but the action of turbulence is not to produce a log-normal distribution.

3. A mathematical model of the breakup process has been developed which allows both the form of the experimentally observed distribution and the kinetics of the breakup process to be simulated. The model provides evidence that each breakup event leads to two daughter drops with uniformly distributed volume ratios and a very small satellite droplet.

4. The existence of a maximum stable drop size is clearly indicated by comparison of various models with experimental data.

5. Tertiary and higher orders of breakup do not appear to be present.

6. Highly distorted drops and breakup appear to be restricted to the neighborhood of the pipe wall.

7. Average drop size increases slowly with distance from the pipe wall.

8. The mathematical model contains three parameters. Sleicher's relationship [Equation (5)] gives a good prediction of the maximum stable drop size. No correlations exist to predict the slope of the straight line which describes the probability of breakup above the maximum stable drop size or to predict the ratio of satellite volume to daughter drop volume. Both of these parameters appear to be system dependent and must be determined by trial and error fit of more extensive experimental data than obtained in this work. In the limit of a very long pipe, the breakup process reaches completion and the form of the model indicates that the slope of the breakup probability function would no longer be a parameter of the distribution at this limit. The

ratio of satellite volume to daughter drop sizes sets the position of the high peak observed at small drop sizes. Best results were obtained if this ratio was set so as to give the mode of the peak at approximately 30 μ for all systems studied.

ACKNOWLEDGMENT

The authors express appreciation to the National Science Foundation for a grant to support research described in this paper.

NOTATION

C, C_1, C_2 = constants
D = drop diameter, L
D_{qp} = weighted average drop size as described in Equation (6), D_{32} diameter obtained with $q = 3$, $p = 2$, L
D_{max} = maximum stable drop diameter, L
D_{95} = diameter below which 95% of the volume is found, L
$D_{1.0}$ = diameter at which probability of breakup becomes 100%, L
F = force
f = arbitrary function in Equation (6)
L = length
M = mass
N_{Re} = Reynolds number based on pipe diameter and continuous phase properties
$(N_{We})_{crit}$ = critical Weber number, $\frac{\rho \overline{v^2} D_{max}}{\sigma}$
N_{Vi} = viscosity group, $\mu_d/(\rho_d \sigma D)^{1/2}$
R = tube radius, L
R_v = range of satellite to daughter drop volume ratios, L
T = time
U = average velocity, L/T
$\overline{v^2}$ = time average value of square of turbulent velocity fluctuation, L/T
y = radial distance from the pipe wall, L

Greek Letters

ε = energy dissipation per unit mass per unit time, FL/MT
μ = coefficient of viscosity, M/LT
σ = interfacial tension, L/T
ρ = density, M/L^3
Ψ = arbitrary function in Equation (1)

Subscripts

c = continuous phase
d = dispersed phase

LITERATURE CITED

1. Adler, C. R., et al., *Chem. Eng. Progr.*, **50**, 14–24 (1954).
2. Clay, P. H., *Koninklijke Nederlandsche Akad. Wetenschappen*, **43**, 852–865, 979–990 (1940).
3. Collins, S. B., Ph. D. thesis, Oregon State Univ., Corvallis (June 1967).
4. Hinze, J. O., *AIChE J.*, **1**, 289–295 (1955).
5. Kinter, R. C., et al., *Can. J. Chem. Eng.*, **39**, 235–241 (1961).
6. Kolmogorov, A. N., *Akad. Nauk U. S. S. R. Dokl.*, **66**, 825–828 (1949). (translated from the Russian).
7. Mugele, R. A., and H. D. Evans, *Ind. Eng. Chem.*, **43**, 1317–1324-(1951).
8. Paul, H. I., and C. A. Sleicher, Jr., *Chem. Eng. Sci.*, **20**, 57–59 (1965).
9. Rumscheidt, F. D., and S. G. Mason, *J. Colloid Sci.*, **16**, 238–261 (1961).
10. Sleicher, C. A., Jr., *AIChE J.*, **8**, 471–477 (1962).
11. Ward, J. P., Ph.D. thesis, Oregon State Univ., Corvallis (1964).

Manuscript received October 8, 1968; revision received July 3, 1969; paper accepted July 7, 1969.

Feedback Control of an Enriching Column

KEITH F. SHONEMAN and JACK A. GERSTER

University of Delaware, Newark, Delaware

The transient behavior of a 24-in. diameter, 10-tray enriching column was investigated experimentally while the column was operated under closed-loop, feedback control. This behavior was compared with that of a perturbated linear model with the column open-loop behavior being represented with simple transfer functions in the frequency domain. Comparisons showed that control parameters determined with the predictive linear model were conservative and permitted stable and smooth responses of the experimental column.

At present, control systems for chemical processes can be well-designed if the process dynamics are known in either the time or frequency domain. For distillation columns, the equations describing the transient behavior are nonlinear. A numerical, nonlinear model in the time domain representing the open-loop behavior has been developed by Huckaba (*5*) and applied to open-loop studies. This and similar numerical methods involve complex numerical techniques which do not provide a simple method of studying the closed-loop behavior for control studies, and are not capable of generalizing the behavior of various columns through steady state parameters. These problems indicate more promise for modeling of the system in the frequency domain.

Simple correlations by Gilliland and Mohr (*6*) and by Pigford (*10*) have attempted to generalize the frequency response using the steady state parameters of the system. At present, however, neither method has been directly applied to control. Rosenbrock (*11*) has developed a complex numerical method employing a discrete variable time to formu-

Dr. Jack A. Gerster is deceased.